NATIONAL RADIO ASTRONOMY OBSERVATORY
GREEN BANK, WEST VIRGINIA

ELECTRONICS DIVISION INTERNAL REPORT NO. 164

140-FT POINTING ERRORS AND POSSIBLE CORRECTIONS

SEBASTIAN VON HOERNER

DECEMBER 1975

NUMBER OF COPIES: 200

140-ft POINTING ERRORS AND POSSIBLE CORRECTIONS

Sebastian von Hoerner

Summary

An investigation of pointing data, obtained astronomically by Kellermann, gave rms errors of 12 arcsec in both hour angle and declination at night, and 13 in HA and 25 in Dec during days, with a maximum of 60 arcsec for the latter. A tentative breakdown for the Dec errors at night gave 8 arcsec for refraction, 5 for thermal deformations, and 7 arcsec as the "intrinsic error" to which all pointing errors could hopefully be reduced if proper corrections were applied using measured atmospheric data for the refraction, and measured structural temperature differences for the thermal deformations.

Individual refraction corrections are suggested which will be installed in December, using data about temperature, pressure and water vapor from the interferometer.

Thermal deformations were monitored during maintenance and longer repair periods, whenever the telescope was not moved, with a total of 27 days and 6 nights. Temperature differences were measured with 8 thermistors on polar shaft and yoke arms, and angular deformations with 4 electronic levels. Good agreement was found between thermally predicted and actually measured deformations. Axial shifts between polar shaft and tail bearings were measured with 2 dial indicators.

The fastest changes measured were 20 arcsec/hour for the Dec error, and 13 for the HA error. The peak to peak range, between extremely sunny days and rain or snow, was 11.5°C for the temperature difference ΔT_a across the polar shaft (see Figure 2b), 8.8°C for ΔT_E across the east yoke arm, and 5.7°C for ΔT_W across the west arm. The concrete platform gets 2.6 mm longer in sunshine than under

snow, thus tilting the polar axis by 21 arcsec peak-to-peak. The ptp range for the measured HA error was 37 arcsec, and 105 arcsec for the Dec error. Using in the future automatic thermal corrections with 8 thermistors, these errors could be reduced by a factor of three. The remaining rms residuals would be 12 arcsec in Dec and about 5 in HA.

The maximum ptp residuals, 34 arcsec in Dec, are still much too large, especially if we want to improve the surface accuracy for shorter wavelengths. For λ = 1 cm, and demanding a pointing error smaller than 1/6 of the beam, we must have errors < 9 arcsec. In addition to thermal corrections, it is suggested to reduce the thermal deformations by shielding polar shaft and southern platform, and by blowing ambient air through the yoke arms.

The influence of the wind was investigated, too. Fast fluctuations are visible already at 10 mph and become serious at 20 mph. But averaged pointing offsets are small and can be neglected up to 30 mph. The wind reduces all temperature differences ΔT, to half their value in calm air, at about v_0 = 12 mph; this thermal smoothing is less effective for the dense, compact 140-ft structure than the one previously measured for thin surface plates (v_0 = 3.8 mph).

I. Astronomical Pointing Data

1. Parameters for Pointing Corrections

The repeatable pointing deviations of a telescope are due to the misalignments of polar and declination axes, and to gravitational deformations. They depend only on hour angle and declination and should be exactly the same for all time. The refraction depends to some extent on weather conditions, but it is treated at present as depending on elevation only, with a constant parameter. In addition, we have an offset of the receiver box which will stay constant during each observation period but will change whenever the box is moved or replaced. All repeatable deviations are taken care of by automatic pointing corrections. On top of these, we have thermal and wind deformations. Thermal deformations could also be corrected for, if we would know exactly where they come from, and if several thermistors (electronic thermometers) were put at the proper places.

Originally, all repeatable deviations were described by nine parameters, A_1 to A_9, to be used for the pointing corrections. A careful investigation of the residuals (Pauliny-Toth 1969) showed that six more parameters were needed. While the old 9-parameter corrections left residuals of about 20 arcsec, the new 15-parameter corrections were found to leave 9 arcsec in RA and 15 arcsec in Dec.

Herrero (1972) investigated analytically the question of how many and which parameters there should be. He found 15 parameters, all identical with the ones found empirically by Pauliny-Toth. Since 1972, the pointing corrections are done automatically and on-line by the computer, using these 15 parameters (Gordon, et al. 1973).

The numerical values of the parameters have been determined by astronomical observations several times. Table 1 shows some results (omitting A_1, A_2 and A_6 which are dial errors and box offsets). The refraction term is A_3; all other

terms result from misalignments of axes and from gravitational deformations. They should not vary with time. Actually, Table 1 demonstrates the considerable uncertainty of defining these parameters. This is caused by the fact that we have only two independent variables, HA and Dec; although their combinations (last column of Table 1) are all different, they are not independent. Thus, different sets of parameters may still give similar residuals.

TABLE 1

Several Determinations of the 12 Constant Parameters.

All parameters are given in minutes of arc.
H = hour angle, D = declination, Z = zenith distance.

	Pauliny-Toth August 1968	Gordon, *et al.* June 1973	"Standard" Kellermann Jan.+March 1975	Three Nights (March 1975)	Angular Dependence
A_3	1.19	1.08	1.04	.95	$\tan Z\ (1 - .0011 \tan^2 Z)$
A_4	.37	2.32	1.54	-2.24	$-\sin H \sec D$
A_5	1.48	22.04	23.14	16.08	$\sin D \cos H \cos L - \sin L \cos D$
A_7	-.40	-1.98	-1.18	-5.34	$-\tan D \sin H + \cos H$
A_8	-.26	-.53	-.52	-.44	$\tan D \cos H + \sin H$
A_9	.93	1.32	1.12	.33	$\tan D$
A_{10}	.50	1.53	.60	7.71	$-\sin H \sin D$
A_{11}	-.19	-2.00	-1.52	1.89	$-\sin H$
A_{12}	-1.58	-16.64	-17.19	-12.22	$\cos H \sin D$
A_{13}	1.53	.24	-.19	-3.66	$\sin D$
A_{14}	-.29	.43	-.93	3.40	$\cos H$
A_{15}	.23	12.72	13.52	-.55	$\cos D$

For illustrating this difficulty, C. Williams took from Kellermann's data a selection of three nights, March 21-24 of 1975, for a new least-squares solution of all 15 parameters, giving rather different results (see Table 1) and smaller residuals. The same three nights were also investigated with the standard parameters. Going from standard to new parameters, the residuals went down from 10.9 to 6.0 arcsec in RA, and from 10.5 to 5.7 arcsec in Dec. But this improvement is completely unrealistic. The three nights contain n = 33 observations, 7 of which turned out to be cases where the operator just used the previous offset instead of scanning the source again, which leaves 26 true observations. But if we solve for 15 parameters, we have only n = 26 - 15 = 11 degrees of freedom. Thus, when calculating the rms residual, we should have divided by $\sqrt{11}$ instead of $\sqrt{33}$. Multiplying the new residuals with a correcting factor of $\sqrt{33/11}$, we now obtain 10.4 arcsec in RA and 9.9 arcsec in Dec, just about the same as with the standard parameters. This clearly shows that a very large number of independent observations is needed for improving the parameters.

2. Single Error Contributions

From Kellermann's data, we took two longer periods of continuous pointing observations, Jan. 13-16 and March 20-24, 1975. The most obvious effect, as already pointed out by Kellermann, is the strong increase of declination errors during the day, probably caused by thermal deformations.

First, we divided the two periods into two parts, night and day (drawing the line at 7:00 a.m. and 19:00 p.m. EST). The residuals from the standard parameters are shown in Table 2. Most significant is the strong increase of the rms declination errors during the day. A closer inspection showed them to be strongly correlated with sunshine, in the sense that the telescope bends north with sunshine. In other periods, not analyzed here, Kellermann finds maximum deviations of -60 arcsec in Dec on clear days.

TABLE 2

Pointing Errors, Night versus Day.

(seconds of arc)

Period	maximum		rms	
	RA	DEC	RA	DEC
Night	+13 -37	+20 -20	12	12
Day	+31 -11	+20 -40	13	25

Second, we ask for a breakdown of the errors at night. If the same source is observed in one-hour intervals, we assume that not much has changed in between. We read the difference between adjacent errors, Δ_i and Δ_{i-1}, and we call $E = (1/\sqrt{2})$ rms $(\Delta_i - \Delta_{i-1})$ the "intrinsic" pointing error. Any time where the observation went from one source to a different one, we have in addition the influence of "bad parameters", including refraction, called P. On top of that we have the thermal deformations, called T, which show up over longer time intervals during the whole duration of the night. We assume that all three contributions add up quadratically. Results of this analysis are shown in Table 3.

TABLE 3

Declination Errors (arcsec), Nights Only.

Method	January 13-14	January 15-16	March 20-21	March 21-24	Average, Contributions
Same source: $\frac{1}{\sqrt{2}}$ rms $(\Delta_i - \Delta_{i-1})$	3.1	6.9	11.4	4.8	6.6 = E
Change source: $\frac{1}{\sqrt{2}}$ rms $(\Delta_i - \Delta_{i-1})$	7.6	8.1	13.9	11.5	10.3 = $\sqrt{E^2 + P^2}$
Whole night: rms $(\Delta_i - \Delta_{aver})$	6.2	14.0	15.5	10.5	11.6 = $\sqrt{E^2 + P^2 + T^2}$
Weather:	rain all night	clear sky	1/4 clouds	partly cloudy, some rain	

From the last column we obtain the single contributions at night in the average as

E = 6.6 arcsec, intrinsic error,

P = 7.9 arcsec, bad parameters including refraction,

T = 5.3 arcsec, thermal deformations.

Also, at night, the thermal deformations are correlated with the weather:

$$T\ (\text{arcsec}) = \begin{cases} 0 & \text{rain all night} \\ 0 & \text{partly cloudy, some rain} \\ 6.9 & \text{sky 1/4 cloudy} \\ 11.4 & \text{clear sky all night} \end{cases} \qquad (1)$$

Because of limited data and simplifying assumptions, this breakdown is only a rough estimate, of course. But still it gives us some hope that future pointing errors may be reduced to their intrinsic part, to E $\approx$ 7 arcsec. For this purpose, we must (a) calculate the proper refraction from measured values of air temperature, pressure and water content; (b) then solve again for all remaining parameters; and (c) correct thermal deformations from measured structural temperature differences.

II. Estimates of Thermal Deformations

The pointing errors must finally be calibrated empirically against measured temperature differences in the structure. But for checking and understanding, we first need some rough estimates. Figure 1 gives the simplified geometry of the main structural parts, and the formulas to be used. For the coefficient of thermal expansion, we use

$$\begin{aligned} C_{th} &= 0.99 \times 10^{-5}/^{\circ}C \quad \text{for concrete,} \\ &\quad 1.17 \qquad\qquad\quad \text{steel,} \\ &\quad 2.30 \qquad\qquad\quad \text{aluminum.} \end{aligned}$$

Looking at the design of foundations and structure, we find that it should never be the temperature itself which matters, but only temperature differences from one part to the other.

1. The Concrete Platform

In general, both the platform and its central tower could expand as well as tilt. Since the measured tilts were only small, ± 2 arcsec, they shall be neglected here; and since the dark-gray platform warms up in sunshine considerably more than the white tower, the latter shall be neglected too.

With Figure 1d, the elongation of the platform, and the resulting tilt of the polar axis are

$$\Delta P = 4.44 \times 10^{-3} \text{ inch/°C}, \tag{2}$$

$$\Delta\theta = 0.99 \text{ arcsec/°C}. \tag{3}$$

Between night and a sunny day, the surface temperature changes considerably, more than 20 °C. But we do not know in which depth we should measure. Instead, we measured ΔL at the gliding tail bearing (subtracting the elongation of the shaft as calculated from its measured temperature change). Then

$$\Delta\theta = 0.284 \text{ arcsec} / 10^{-3} \text{ inch}. \tag{4}$$

2. Polar Shaft Bending

First, we consider the shaft as having the same ΔT all over its exposed length. From Figure 1b we find for the tilt, at both ends,

$$\Delta\theta = \frac{1}{2}\frac{L}{d} C_{th} \Delta T = 4.22 \text{ arcsec/°C}. \tag{5}$$

Second, the southern half of the shaft is almost completely filled with concrete giving a very long time delay, while the northern half if empty. This results in different ΔT, for the near and the far part, as seen from an end. A detailed calculation gives for this case

$$\Delta\theta = 4.22 \text{ arcsec } \frac{3\ \Delta T_{near} + \Delta T_{far}}{4} . \qquad (6)$$

The actual tilt, however, is the sum of this bending and the platform elongation.

3. York Arm Bending

The yoke arms are mostly less (and more symmetrically) exposed to sunshine than the shaft. But in addition, the platform surface and the ground warm up a good deal and then radiate infrared which is well absorbed by the protective paint on the yoke (white in the visible, but black in the infrared). We apply Figure 1c and obtain, for steel,

$$\Delta\theta = 10.1 \text{ arcsec/°C.} \qquad (7)$$

We see that even small temperature differences give large tilts at the upper end of the yoke arms. (Comparing Figures 1c and 1b, there is a factor of two if one end is fixed.)

4. Backup Structure

Temperature differences at the declination wheel would not matter for actual pointing errors. But during the monitoring to be described later, both brakes are set. If one half of the wheel now warms up more than the other, we obtain from Figure 1e a tilt of the axis against the yoke, to be measured at the declination readout at the console:

$$\Delta\theta = C_{th}\ \Delta T = 4.74 \text{ arcsec/°C.} \qquad (8)$$

Another item matters for the pointing but is not monitored at present. This is the bending of the cantelevering outer half of the dish. From Figure 1a we find Δz, and a division by the telescope radius then gives a tilt of

$$\Delta\theta = 5.34 \text{ arcsec/°C.} \tag{9}$$

If this were the same all around the telescope rim, it would affect the focusing but not the pointing. A pointing error results if opposite parts of the rim deform by different amounts.

5. Feed Support Legs

If opposite legs have different temperatures, the feed box is moved sideways by Δx, and the resulting pointing error is from Figure 1e

$$\Delta\theta = 5.84 \text{ arcsec/°C.} \tag{10}$$

The results of these estimates are summarized in Table 4. For illustration, we have picked some temperature differences which we assume to be typical for sunny days; they are mainly based on measurements done years ago (at somewhat different locations). During nights, we expect the differences to be about 1/6 of those used in the table. Comparing the results with the measured pointing errors of Table 2 and equation (1), it seems that we have indeed obtained the right magnitude.

TABLE 4

Various Thermal Contributions to Declination Pointing Errors.

Item	Material	Arcsec/°C	Assumed ΔT sunny days °C	$\Delta\theta$ arcsec	Direction at noon
Platform elongation ..	Concrete	.99	8	8	N
Shaft bending	Steel	4.22	5	21	N
Yoke arms	Steel	10.1	4	40	N
Rim cantelever	Aluminum	5.34	1.5	8	N
Feed legs	Aluminum	5.84	1.5	9	S

6. Hour Angle Error

a) Shaft bending, EW. Before noon on sunny days, the east side of the polar shaft will be warmer by ΔT_d (see Figure 2b) than the west side. The rotation angle of the sphere then is 4.22 ΔT_d arcsec, from equation (5), and in stow position this angle is projected on the vertical plane with a projection factor of sin β = 0.621:

$$\Delta_1 = 4.22\ \Delta T_d \sin\beta = 2.62\ \Delta T_d. \qquad (11)$$

b) Yoke elongation difference. Before noon, the east yoke arm will be warmer than the west arm by ΔT_{EW}, yielding a lift of the east bearing in proportion to $C_{th}\ \Delta T_{EW}$. Calling Y the arm length of the yoke, and A the length of the declination axis, we find from Figure 2a and 2b for zenith position

$$\Delta_2 = (Y/A)\ C_{th}\ \Delta T_{EW} \cos\alpha = 1.94\ \Delta T_{EW}. \qquad (12)$$

c) Yoke bending difference. If the south side of the east arm is ΔT_E warmer than its north side, the top of the east arm tilts north by 10.1 ΔT_E according to equation (7), and the connecting line between top and sphere tilts by half this angle. Since this connecting line is not vertical, the top of the east yoke arm will be slightly raised, by an amount Y (1/2) 10.1 ΔT_E sin α. In a similar way, the top of the west arm will be raised in proportion to ΔT_W. And if both tops are raised by different amounts, the resulting hour angle error will be in zenith position.

$$\Delta_3 = (Y/A)\ (1/2)\ 10.1\ (\Delta T_E - \Delta T_W) \sin \alpha = 1.69\ (\Delta T_E - \Delta T_W). \qquad (13)$$

TABLE 5

Thermal Contributions to Hour Angle Error.

Item	Arcsec /°C	Assumed ΔT, °C sunny morning	Δ HA arcsec	Direction morning
Shaft bending	2.62	4	10	W
Yoke elongations	1.94	3	6	W
Yoke bearings	1.69	3	5	W
Rim cantelever	5.34	1	5	W
Feed legs	5.84	1	6	E

Table 5 summarizes all contributions. The temperature differences are assumed smaller for the HA error than in Table 4 for the DEC error, because morning and evening sun are less effective than the noon sun.

III. The Refraction

1. Suggested Corrections

Up to now, the refraction has been treated as a time-independent term,

$$r = A_3 \, (1 - 0.0011 \tan^2 Z) \tan Z \qquad (14)$$

with A_3 = 1.04 arcmin = 62.4 arcsec for the standard values of Table 1. The refraction would just go with tan Z if the surface of the Earth were an infinite flat plane. The term in parenthesis is a correction for the actual surface curvature, but it is only an approximation, which gets unreliable below about 10° elevation and breaks down completely below about 5°. As compared to some of the other parameters in Table 1, it would seem that A_3 is not a very large term; but it is multiplied with tan Z and thus becomes very large for small elevations; see the second column of Table 6. This means that the refraction should be dealt with in more detail.

Herrero (1972) gives the dependence of the refractive index n on atmospheric conditions as

$$(n - 1) \, 10^6 = \frac{103}{T} P_d + \frac{86}{T} P_w \left(1 + \frac{5750}{T}\right) \qquad (15)$$

where T = temperature in °K, P_d = dry air pressure in mmHg, and P_w = water vapor pressure in mmHg. The total air pressure is $P = P_d + P_w$. The refraction then is, including the curvature correction, approximated by equation (14) with

$$A_3 = (n - 1). \qquad (16)$$

For a "normal" atmosphere of T = 20 °C = 293.15 °K, with a water vapor pressure of P_w = 8.9 mmHg (50 percent humidity), and a total pressure of P = 760 mmHg, equation (15) yields, in agreement with Table 1,

$$A = 1.092 \text{ arcmin} = 65.5 \text{ arcsec.} \tag{17}$$

Following Herrero, we derive from equation (15) the dependence of the refraction on atmospheric changes from their normal values as

$$\begin{aligned} \partial A_3/\partial T &= -0.260 \text{ arcsec/°C}, \\ \partial A_3/\partial P &= +0.073 \text{ arcsec/mmHg}, \\ \partial A_3/\partial P_w &= +1.248 \text{ arcsec/mmHg}. \end{aligned} \tag{18}$$

TABLE 6

The Normal Refraction r, and Its Change Δr with Atmospheric Conditions.

Elevation degrees	r arcsec	Δr (arcsec)			
		ΔT = 20 °C	ΔP = 20 mmHg	ΔP_w = 6 mmHg	Total (RSS)
45	66	5	1	8	9
30	114	9	2	13	18
20	180	14	4	21	26
10	361	29	8	41	51
5	645	51	14	74	91

Table 6 gives some examples of this dependence, using larger (but not extreme) deviations of temperature and pressure from their normal values. We see that the water vapor is the most important item. The total Δr is calculated as the quadratic sum of the three contributions. The atmospheric corrections should not be neglected for elevations below about 45°. They become very large at 10° elevation, and below this, we consider them as unreliable because then we look through far-away parts of the atmosphere, too, with unknown properties.

From equations (17) and (18) we derive the following formula

$$r = A_3 \tan Z \, (1 - 0.0011 \tan^2 Z) \, K \qquad (19)$$

with

$$K = 1 - 0.00397(T-20°C) + 0.00111(P-760 \text{ mmHg}) + 0.01905(P_w - 8.9 \text{ mmHg}) \qquad (20)$$

We suggest to use this formula for future pointing corrections. We further suggest to leave A_3 still as one of the 15 parameters to be solved for in a future pointing calibration, because it may actually be a little different from the value of equation (17). Also, it may depend somewhat on the wavelength of observation.

2. The Present State

Originally, it was intended to check with Kellermann's previous pointing data (using weather information from the interferometer log sheets) whether the K-term of equation (20) would actually give an improvement over equation (14). Claude Williams collected all available data but found, unfortunately, that during the few longer pointing runs the weather had not changed enough to show the difference. Thus, an observational check on equation (20) must wait for future pointing observations.

Meanwhile, Ron Weimer and Tom Cram have set up an automatic treatment of the K-term. The data about temperature, total pressure, and water vapor pressure are obtained at the interferometer and are transferred in analog form to the 140-ft, where they are converted to digital form. The pointing program of the computer then uses equations (19) and (20), instead of the old equation (14). The curvature term, containing $\tan^2 Z$, has not been changed, and its limitations should be kept in mind.

It was estimated that the K-term should not change by more than 30% even under extreme weather conditions. Thus, as a safety limit, just in case that something breaks down, the computer will make a decision:

$$\text{If} \quad |K - 1| \geq 0.3, \quad \text{then set} \quad K = 1, \quad \text{and print error message.} \qquad (21)$$

The final installment of this automatic treatment is planned for December 17, 1975, and will be used from then on.

IV. Monitoring the Thermal Deformations

1. The Scope

In order to provide future thermal pointing corrections, we need actual measurements of the pointing errors and their single contributions, and we ask for the correlation of these contributions with simultaneously measured structural temperature differences.

Deformations were measured in terms of angular tilts with electronic levels, during days and longer periods of maintenance where the telescope was not moved, with both brakes set. Temperatures were measured with thermistors at 10 different locations. Mounting and cabling of all levels and thermistors was done by Fred Crews and John Ralston.

As the location most representative for the telescope pointing, we have chosen the point at the very center of the backup structure, right above the middle of the declination axis, where a total of 15 heavy members meet in a single joint. Level A (East-West) and Level B (North-South) were mounted there. The present section covers all deformations between this point and the platform, but it neglects the deformations higher up, from the cantelevering rim and the feed legs. Both are difficult to monitor, but they are supposed to be smaller and partly cancelling each other; see Tables 4 and 5.

2. Readings and Ranges

Figure 2b shows the location of 10 thermistors, 4 electronic levels, and 2 dial indicators on the 140-ft; it also gives the definitions of 6 temperature differences ΔT. In addition, we read Dec and HA at the console, ambient air temperature, and wind velocity and direction. Notes are also taken about sky coverage and precipitation, which then were converted to the following scale:

$$\text{sky} = \begin{cases} -1 & \text{light rain or snowfall} \\ -2 & \text{heavy rain or snowfall} \\ 0 & \text{dark overcast} \\ 1 & \text{light overcast} \\ 2 & \text{mostly overcast, or strong haze} \\ 3 & \text{some clouds, or light haze} \\ 4 & \text{clear sky} \\ 5 & \text{very clear dark sky} \end{cases} \qquad (22)$$

Table 7 gives a summary about all 27 days and 6 nights where any readings were taken. This covers 14 normal maintenance days, 5 days of longer installation work (Nov. 15 to 19), and 2 long periods of 3 and 5 days each, including the nights (Aug. 4-6 and Nov. 10-14). Readings were taken with various degrees of completeness. Table 7 gives the peak-to-peak ranges of all readings during each day or period; these ranges depend on the duration of the measurements, and on the clearness of the sky.

Regarding the weather, we had no luck for a long time: of the 16 days from April through October, there was not one day with complete sunshine. But this was made up by the period of Nov. 10-14, with one exceptionally clear day between clear nights, followed by a completely rainy day and one full day of snowfall (covering the whole year, so to say), which is emphasized in Table 7 by the very large ranges measured for this period. The following five single days were also

TABLE 7

Monitoring Thermal Deformations during Maintenance Periods, with Both HA and DEC Brakes Set.

For location of levels and thermistors, see Figure 2b.
Values given are peak-to peak ranges; for air and temperature differences in °C; for levels, DEC and P in arcsec. (P = tilt of polar shaft caused by elongation of concrete platform.)

Day	Duration Hours	Weather		Shaft Temperature Difference			Yoke Arms Temperature Difference			Dec	Electronic Levels				Dec Error	P
		Sky Min.	Sky Max.	Ambient Air	ΔT_a	ΔT_b	ΔT_d	ΔT	ΔT_W	ΔT_{EW}		A	B	C	D	B-Dec	
Apr. 2	3	4		2							6		8			7	
9	5	4		16							4		22			26	
15	5	0		2							6		12			6	
May 7	8	4		11							5		30			26	
21	8	3	4	9	2.9						14		17			21	
Jun. 11	6	0		2	1.0						0		1			1	
July 23	8	0	2	9	2.0						8		10			9	
30	6	2	3	5		2.2					3		13			16	
Aug. 4-6	50	-2	3	12		2.9					13		25			26	6
13	6	2	3	8	3.6	2.3		.8	.6	.7	4		8		20	19	4
20	4	2		11	3.1	2.0		.5	.7	1.0	3						2
Sep. 2	6	1	4	9	5.6	3.6		1.0	1.4	.6	7			13	25		6
17	7	0	3	8	3.8	2.5		1.3	.6	.7	8		17	12	16	9	6
Oct. 8	7	-1	0	8	1.8	1.0		.5	.6	.5	10	10	5	2	5	6	8
Nov. 10-14	89	-2	5	19	11.5	6.7		8.8	5.7	3.7	39	37	99	37	90	105	21
15	11	5		15							33	22	28			52	
16	11	5		9							29	16	42			63	
17	11	5		20							39	33	50			70	
18	11	5		23	10.2		4.9	8.7			40	23	47	27		63	
19	13	5		19	10.3		4.8	7.6			35	18	43	26		67	
22	7	0		2	.7		.2	.3	.3	.2	1	6	10	5		11	

very clear, but temperature measurements were not taken because the morning temperatures were below zero which, unfortunately, could not be measured with the available equipment, and thermistor 9 was out of order.

Not shown in Table 7 are the following:

(a) The hour angle readout at the console, because it always stayed practically constant, never changing more than $0.2^s = 2.4$ arcsec at zenith.

(b) During August 4-6, we also measured the temperature at the top and the bottom of the spherical bearing, both of which stayed constant within 1.2 °C, yielding negligible deformations.

(c) During the same period, we tried to measure a north-south tilt of the tail bearing with a clinometer, but it stayed constant within its accuracy of ± 2 arcsec.

During clear, sunny days, some fast changes may occur. The following gives the fastest changes encountered, and the hour of this maximum change:

Change of	arcsec/hour	Time (EST)
Dec	12	13:00
Level C	6	10:30
Level D	20	9:30
Dec Error (B-Dec)	20	12:00 and 16:30
HA Error (A-HA)	13	9:30 and 13:30

(23)

3. Platform and South End of Polar Shaft

The two dial indicators (Figure 2b) give axial shifts between shaft and tail bearing. Their average, $I_{av} = \frac{1}{2}(I_1 + I_2)$, measures the elongation of the platform minus that of the shaft, and the latter can be obtained from the length of the shaft and its measured average temperature T_{av}. We then calculate the tilt angle P of the polar axis resulting from the elongation of the platform. Omitting the details, we find

$$P = 0.284\, I_{av} + 1.67\, T_{av} \qquad \begin{array}{l} P \quad \text{in arcsec (+ is North tilt)} \\ I_{av} \quad \text{in 0.001 inch} \\ T_{av} \quad \text{in °C} \end{array} \qquad (24)$$

The difference, $\Delta I = I_2 - I_1$, measures the tilt of the southern shaft end (neglecting any tilt of the bearing). The difference between this tilt and the axial tilt P then is the observed bending of the southern shaft end. The predicted thermal bending is obtained from equation (6). Counting a southward bend as positive, we obtain

$$\text{South shaft bending} \begin{cases} \text{observed} = 3.46\, \Delta I + P & (25) \\ \text{predicted} = 4.22\, \Delta T_S & (26) \end{cases} \quad \text{(+ is South bending)}$$

$$\Delta T_S = \frac{1}{4}(\Delta T_a + 3\, \Delta T_b). \qquad (27)$$

Figure 3c shows the platform elongation, contributing a peak-to-peak of 9 arcsec to the declination error, well correlated with sunshine and air temperature, but delayed by 2-3 hours. On very clear days versus rain and snow, the platform even contributes up to 21 arcsec; see Figure 4g.

Figure 3d gives the thermal bending of the southern part of the polar axis. The observed bending is well correlated with the thermally predicted one, but has a smaller amplitude and is delayed by about 2 hours for fast changes and about 6 hours for slow ones. This delay will be caused by the thick concrete filling of the southern part of the shaft.

We find that the platform contributes up to 21 arcsec pointing error, and that the south part of the shaft bends with a delay of some hours. Furthermore, we have neglected any thermal deformations of the concrete tower holding the spherical bearing. All three items would be extremely difficult to measure thermally for pointing corrections. We thus draw the conclusion:

> Polar shaft, south end of platform, and south side of the tower should be shielded against sunshine and rain, and should all be kept at the same (only slowly varying) temperature. (28)

4. Bendings of the Polar Shaft and Yoke Arms

The readings of Dec and four levels are shown in Figure 4c-f, as functions of time for the lucky period of Nov. 10-14. Not shown is the HA reading which never changed more than 2 arcsec. Regarding levels A and B as being representative for the telescope pointing, we then have the observed pointing errors

$$\text{Dec error} = B - \text{Dec}, \tag{29}$$

$$\text{HA error} = A - \text{HA}. \tag{30}$$

In the following, we neglect the influence of platform and tower for the reasons given before conclusion (28). The observed N-S bendings then are

$$\text{Shaft bending} = C, \tag{31}$$

$$\text{Yoke bending} \begin{cases} \text{East arm} = D - C, & (32) \\ \text{West arm} = B - \text{Dec} - C. & (33) \end{cases}$$

These observed bendings shall now be compared with the termally predicted ones. For the shaft, we neglect again its south part, using equation (5) instead of (6); for the yoke arms we use equation (7).

This is done in Figure 5 for the shaft bending. We see a fairly good correlation between observed and predicted bending, plus some residual scatter. The best-fitting slope is not 1.0 but only 0.84, which means that our measured ΔT_a of Figure 2b is larger than the average ΔT along the shaft. This empirical factor 0.84 will be used in the following sections. With 0.84 x 4.22 = 3.54 we find, in arcsec:

$$\text{Shaft bending} = 3.54\ \Delta T_a \pm 4.0 \text{ rms } (8.0 \text{ max}). \tag{34}$$

The large systematic deviations at night, clear sky versus rain and snow, could not be accounted for with available measurements. They probably arise from the tower and deeper parts of the platform, supporting conclusion (28).

The yoke bendings are shown in Figure 6. The best-fitting slope is here 1.0, meaning that ΔT_E and ΔT_W of Figure 2b indeed represent the average ΔT along the yoke arms, in the average over all encountered weather conditions. We find

$$\text{Yoke arm bending} = 10.1\ \Delta T_{E(W)} \pm 7.9 \text{ rms } (28 \text{ max}). \tag{35}$$

The large scatter means that different parts of an arm may have quite different ΔT on different weather conditions, leading to the conclusion:

Either we need more than two thermistors per yoke arm (6, say), or any large ΔT should be avoided, for example, by blowing ambient air through the arms, or by wrapping some thermal insulation around the arms, or both. (36)

Finally, Figure 7 gives the difference, east arm bending minus west arm bending, observed versus predicted. The large scatter is very obvious.

V. The Pointing Errors

1. Observed Errors and Thermal Predictions

The observed pointing errors, as defined in equations (29) and (30), are shown as a function of time in Figure 8, for several days, all errors being set to zero at 8:00 each morning. During sunny days, the declination error may rise by almost 80 arcsec between 8:00 and 16:00, and the hour angle error may change by 26 arcsec between 12:00 and 16:00.

How much of these errors could be removed by future automatic thermal pointing corrections, with the present setup of 8 thermistors? For the thermally predicted declination error, to be used as a correction, we combine equation (34) for the shaft bending with equation (35) for the west yoke arm whose top is the reference for the declination readout at the console:

$$\Delta \text{ Dec predicted} = 3.54\ \Delta T_a + 10.1\ \Delta T_W. \tag{37}$$

For the hour angle correction, we use equation (11) with the empirical reduction factor 0.84 found in Figure 5, combined with the unreduced equations (12) and (13) for the contributions from yoke elongation and bending:

$$\Delta \text{ HA predicted} = 2.20\ \Delta T_d + 1.94\ \Delta T_{EW} + 1.69\ (\Delta T_E - \Delta T_W). \tag{38}$$

The declination error, observed versus predicted, is shown in Figure 9. During the long period of Nov. 10-14, the peak-to-peak range is 105 arcsec. Subtracting the thermally predicted error (straight line), the remaining residual is 34 arcsec peak-to-peak, giving an improvement of

$$\text{Dec error improvement factor} = 105/34 = 3.09. \tag{39}$$

The residuals (observed - predicted) are

$$\text{rms (Dec residuals)} = 12 \text{ arcsec (89 hours, with sun, rain, snow).} \tag{40}$$

The hour angle error is shown in Figure 10 for two sunny days (no nights with predictions available). The peak-to-peak ranges are 26 arcsec for the observed errors, and 8 arcsec for the residuals, giving

$$\text{HA error improvement factor} = 26/8 = 3.25. \tag{41}$$

For the residuals we obtain

$$\text{rms (HA residuals)} = 2.2 \text{ arcsec (2 sunny days, 11 hours each),} \tag{42}$$

which would be increased probably to about 5 arcsec if we could have also included nights, rain and snow. The three contributions to the HA error are shown in Figure 10b; they are all of comparable size.

2. Future Thermal Corrections

The outputs of the eight thermistors should be converted to digital form and fed into the on-line computer, where the following five temperature differences are calculated: ΔT_a, ΔT_d, ΔT_E, ΔT_W and ΔT_{EW}. (See Figure 2b for

definitions.) Which thermal pointing corrections should now be applied, in addition to the 15-parameter corrections of Table 1 and the detailed refraction correction of equation (20), for any given declination and hour angle of the telescope? Up to now, all our equations were derived for zenith (stow) position only.

Since all thermal readings just rotate with the telescope in hour angle, no dependence on the hour angle can occur for equations (37) and (38). Furthermore, since equation (37) does not contain any declination-dependent projection factors, it cannot change with declination, either. This is different for the hour angle correction, where its three contributions enter with different projection factors; see equations (11), (12), and (13). For any given telescope pointing, we now obtain, where (15-par.) means the old 15-parameter pointing correction,

$$\text{Dec(corr.)} = \text{Dec(15-par.)} + 3.54\ \Delta T_a + 10.1\ \Delta T_W; \tag{43}$$

$$\text{HA (corr.)} = \text{HA (15-par.)} + 3.54\ \Delta T_d \sin(\text{Dec}) + 2.10\ \Delta T_{EW} \cos(\text{Dec}-15.9°) + 4.42\ (\Delta T_E - \Delta T_W)\ \sin(\text{Dec}-15.9°). \tag{44}$$

All ΔT are to be measured in °C, and corrections (43) and (44) are both calculated in seconds of arc. If the hour angle correction is wanted in seconds of time, then its three terms must all be divided by 15 cos(Dec).

3. Wind-Induced Pointing Errors

Stronger winds should give pointing errors increasing with the square of the wind velocity and depending on its direction. Looking at the readouts of console and levels, one sees that medium winds give considerable fast fluctuations, but only little average offsets. Although the 140-ft structure is very

heavy and resists bending, some dynamical resonances seem to get excited more easily. Our present data are very scanty, and new measurements in stronger winds would be needed for reliable results.

The average offset is investigated in Figure 11 during a period of 50 hours which was thermally relatively quiet, with occasional winds of 20 mph. The hour angle data cannot be evaluated since the wind showed no strong EW component. Figure 11d asks for a correlation between the residual declination error and the square of the north wind velocity. The scatter is too large for giving a significant correlation, the result being only

$$\text{Dec residual (observed-predicted)} = (2 \pm 3)\ \text{arcsec} \left\{ \frac{v}{20\ \text{mph}} \right\}^2 . \qquad (45)$$

Thus, the pointing averaged over some minutes is not seriously degraded up to 30 mph.

The fluctuations were not really investigated. An eye inspection shows them to be already obvious at 10 mph, and for our strongest winds we found about

$$\left.\begin{array}{l} \pm\ 5\ \text{arcsec in HA (level A)} \\ \pm\ 20\ \text{arcsec in Dec (level B)} \end{array}\right\} \quad \text{at 20 mph.} \qquad (46)$$

4. Thermal Smoothing from Wind

Stronger winds should prevent or smooth out any larger structural temperature differences ΔT by bringing all temperatures closer to that of the ambient air, which should decrease the thermal pointing errors. In Report 36 (von Hoerner 1971) for our 65-m design, we tried to investigate this effect and estimated a dependence of the form

$$T(v) = \frac{\Delta T_0}{1 + v/v_0} . \qquad (47)$$

Measurements were taken with a surface plate of thin aluminum sheet in sunshine with its rib structure underneath in shadow, blowing air at various speeds horizontally with ventilators. Equation (47) seemed to be fulfilled, and v_0 was found as $v_0 = 3.8$ mph.

For a similar investigation on the 140-ft, we take six extremely and equally sunny days (Nov. 11, 15, 16, 17, 18, 19) with 11 hours duration each. The readings of Dec, levels A and B were plotted over time; see Figures 12 a, b, and c for two of these days. For each case, a "zero" line was drawn from the value at 8:00 to that at 19:00 EST. The deviations Δ from this line were read at the average occurrence of their maxima: at 12:00 for all ΔA, at 14:00 for ΔB, at 11:30 for the max of Δ Dec, and at 15:30 for its minimum. We expect again $\Delta = \Delta_0/(1 + v/v_0)$; Δ_0 was obtained as the average Δ for all $v \leq 2$ mph; and v was taken as the average velocity of the 4 previous hours (for example, at 8, 9, 10, 11 EST for level A; at 10, 11, 12, 13 EST for level B). From equation (45) we then expect Δ_0/Δ to increase linearly with v, the slope being $1/v_0$. Figure 11d shows indeed some correlation, but with a large scatter. The result is about

$$v_0 = 12 \text{ mph} \tag{48}$$

for that wind velocity where all ΔT are reduced to half their values in calm air. This v_0 is about three times larger than the old one from the surface plates. Maybe this shows the difference between a thin sheet being equally well cooled on both sides in our old setup, and a heavy I-beam with one half in its own wind shadow. Also, all leeward members of the 140-ft are in the wind shadow provided by the rather dense telescope structure.

Acknowledgements

It is a pleasure to thank Fred Crews for his untiring help and initiative regarding the instrumental setup and the readings; John Ralston and Sidney Smith for assisting Fred, and for digging out all structural information needed; Tom Cram and Ron Weimer for installing the refraction corrections and preparations for thermal corrections; Claude Williams for analyzing the astronomical data, and Ken Kellermann for providing them.

References

Gordon, M A., Huang, S., Cate, O., Kellermann, K. I., Vance, B.: "On-Line Pointing Corrections of the 140-ft Telescope", Telescope Operations Division Report No. 11; June 15, 1973.

Herrero, V.: "140-ft Telescope Pointing Calibration"; April 25, 1972.

Hoerner, S. von: "Thermal and Wind Deformations of the Surface Plates", Report No. 36; June 20, 1971.

Pauliny-Toth, I.: "Pointing Corrections for the 140-ft under Computer Control", Memo; May 7, 1969.

a) Slender truss, one end fixed:

$$\Delta z = \frac{L^2}{h} C \Delta T$$

b) Long tube, ends supported:

$$\Delta\varphi = \frac{1}{2}\frac{L}{d} C \Delta T$$

c) Long tube, one end fixed:

$$\Delta\varphi = \frac{L}{d} C \Delta T$$

d) Elongation of platform:

$$\Delta P = P C \Delta T$$

$$\Delta\varphi = C \Delta T \sin\varphi \cos\varphi$$

$$\Delta L = \Delta P \cos\varphi$$

e) Triangle, base fixed:

$$\Delta x = \frac{h^2 + b^2}{2b} C \Delta T$$

$$\Delta\varphi = \Delta x / h$$

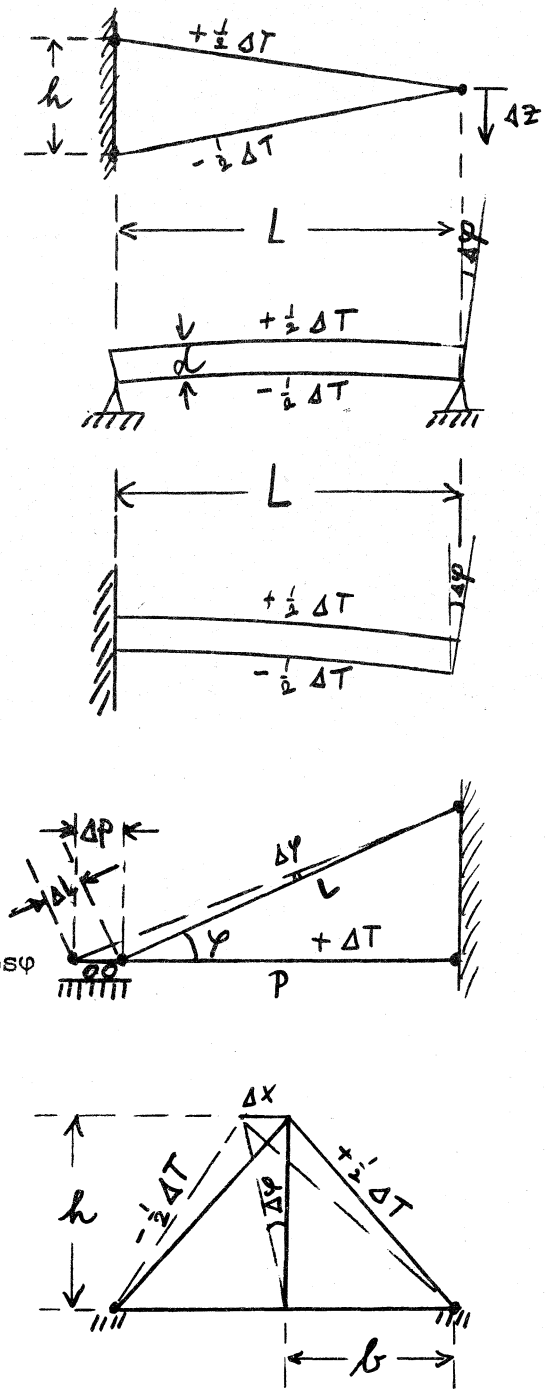

dish rim:
h = 12.1
L = 30.9

polar shaft:
L = 42
d = 12

yoke arms:
L = 42
d = 10

polar axis:
P = 37.6
φ = 38.4°

declination wheel:
h = b = 35.5

feed legs:
h = 62.7
b = 32.1
} in projection

Fig. 1. Geometry, for estimates of thermal deformations.

All lengths are given in feet; C = coefficient of thermal expansion.

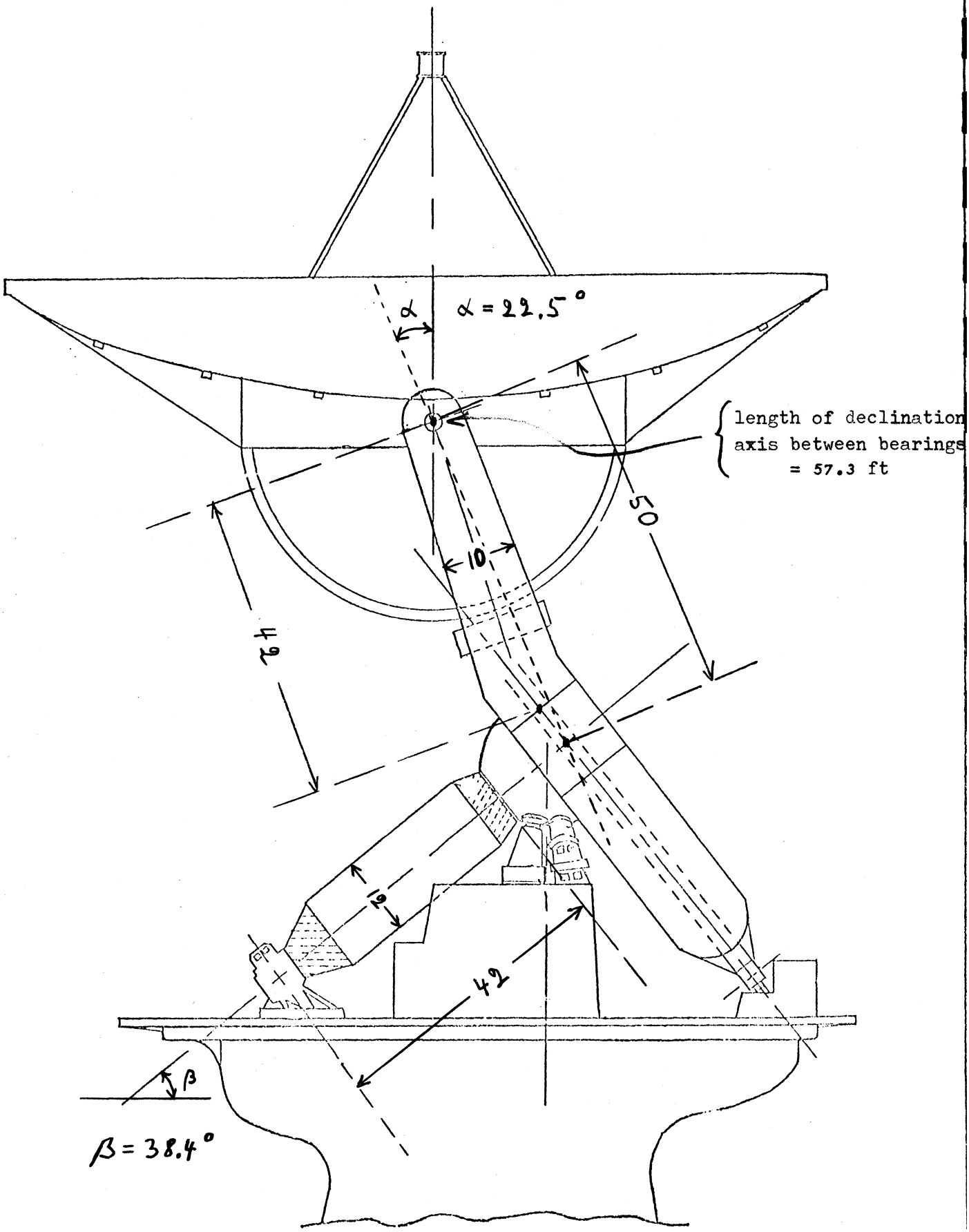

Fig. 2a. Dimensions (feet) and angles of 140-ft.

α = average yoke arm versus vertical,

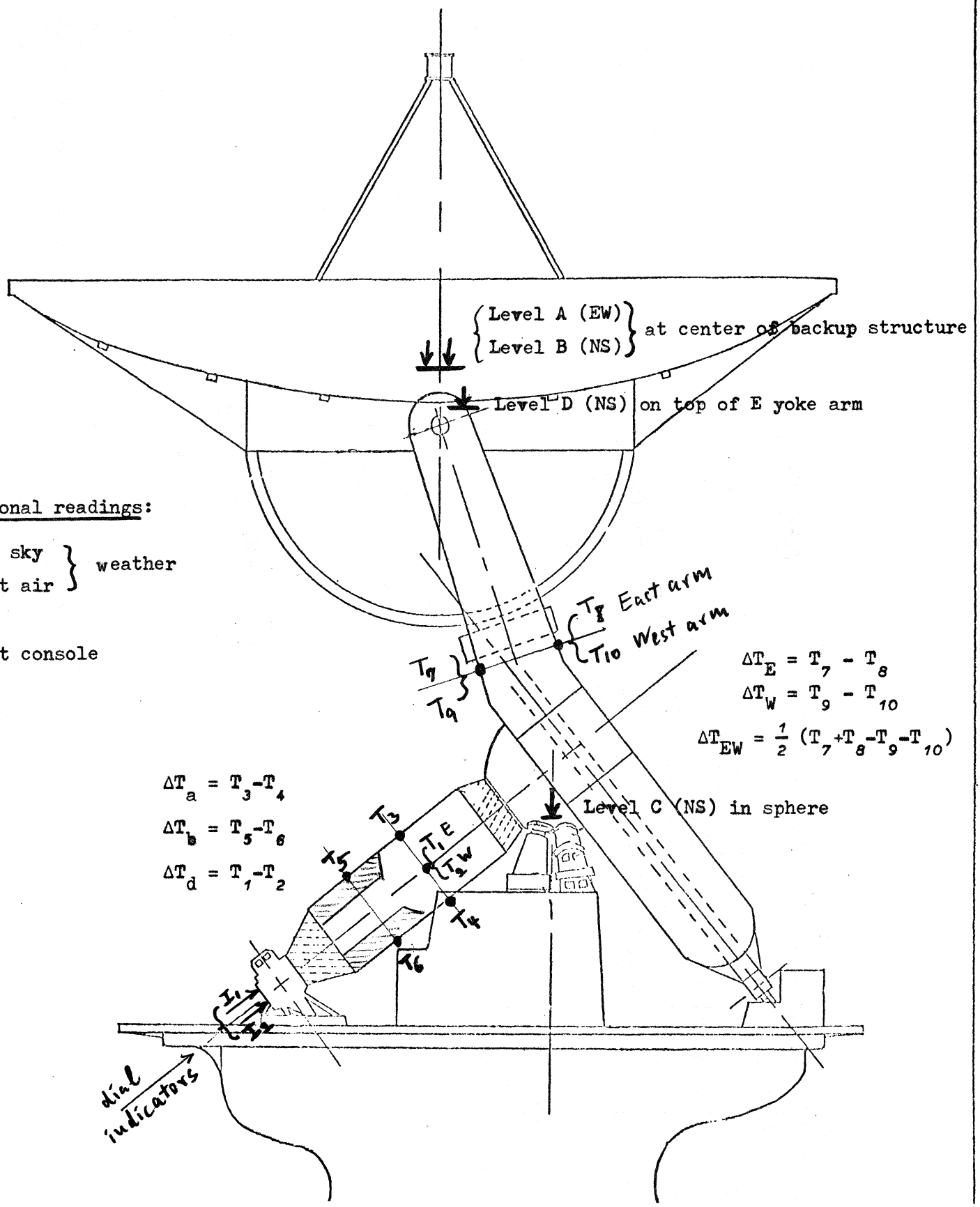

Fig. 2b. Readings taken at the 140-ft.

The dial indicators, and electronic levels A, B, C, D, are read only in stow position (zenith), with both Dec and HA brakes set. The dial indicators are fixed on the shaft, 59.5 inch apart, pushing against the bearing.

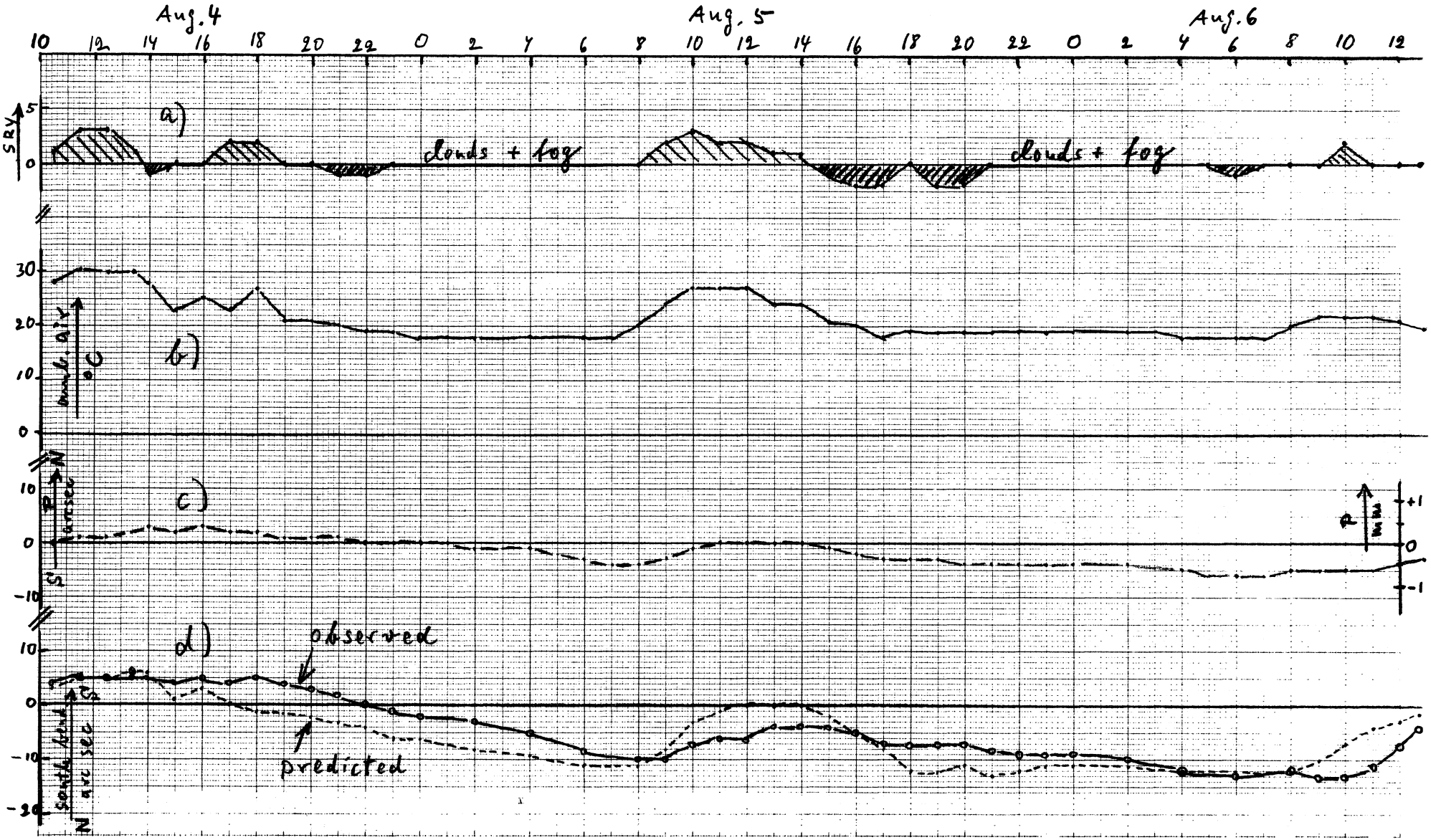

Fig. 3. Platform and southern end of polar shaft, Aug. 4 - 6. a) and b) Weather data.

c) Elongation P of concrete platform, right-hand scale in mm; resulting tilt of axis, left-hand scale.

d) Thermal bending of southern shaft end; $\begin{cases} \text{observed} = 3.46\ \Delta I + P, \\ \text{predicted} = 4.22\ \Delta T_S. \end{cases}$

Fig. 4. Long run with both brakes set, Nov. 10–14, 1975. Plotted over time: Weather (sky, ambient air, wind); declination reading; 4 electronic levels, A, B (in backup structure), C (in sphere), D (on east yoke top); platform.

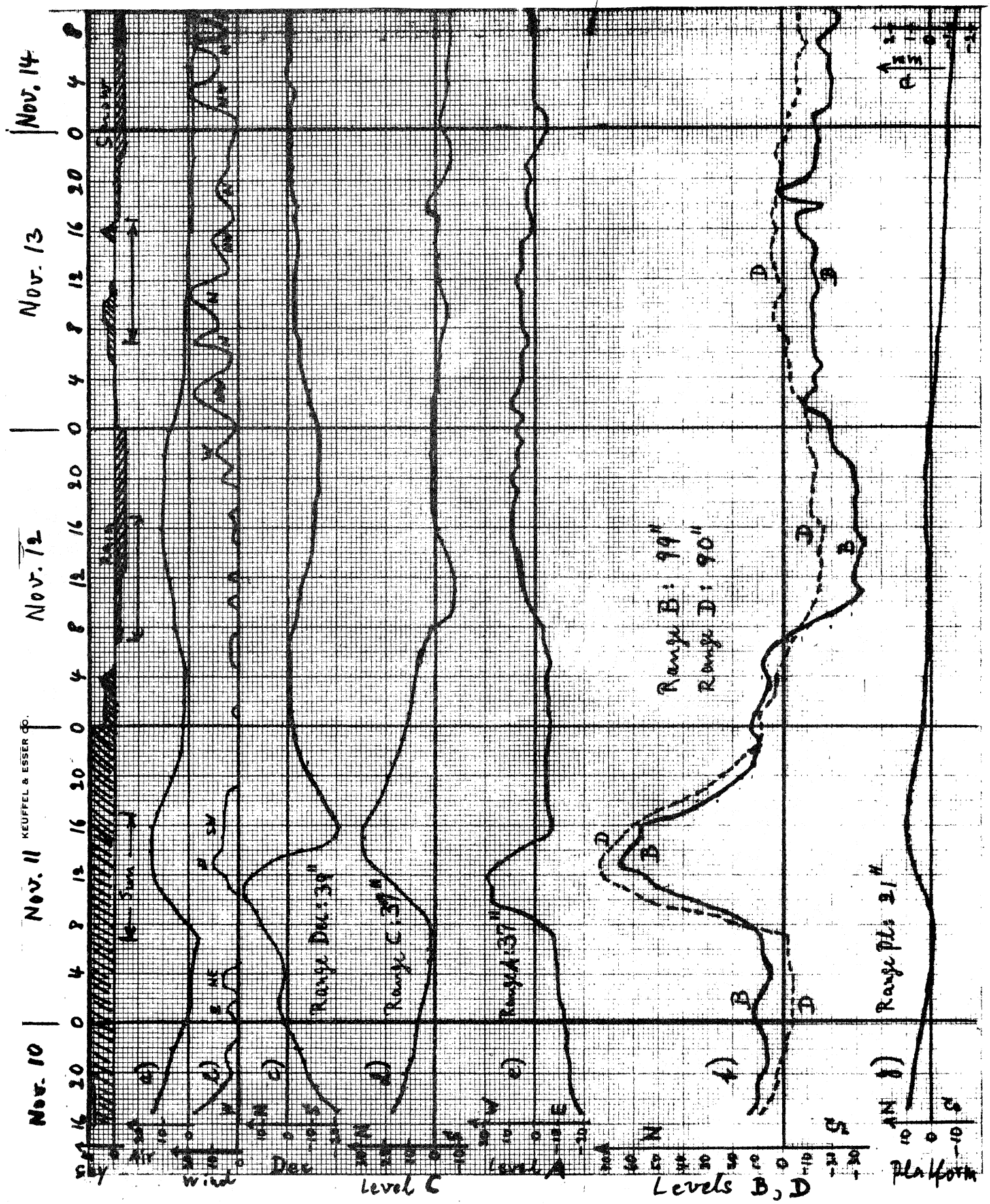

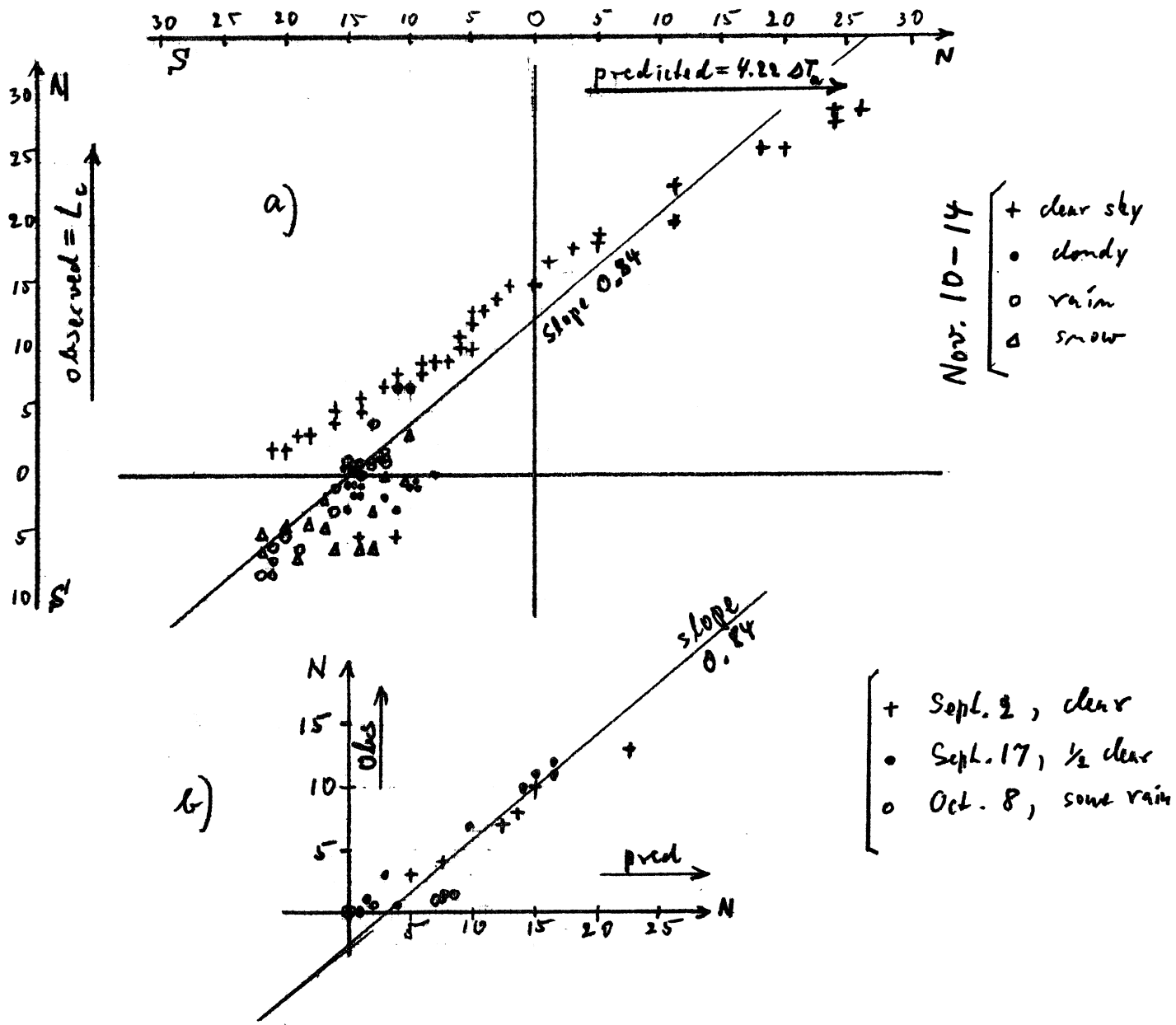

Fig. 5. Tilt angle of the spherical bearing (arc sec);
predicted: from temperature difference ΔT_a in upper shaft,
observed: electronic level C, mounted in the sphere.

a) Nov. 10-14 (89 hours); zero of level C is arbitrary, but the same throughout.

b) Three maintenance days (6-7 hours each); both scales are set to zero at the start of each day.

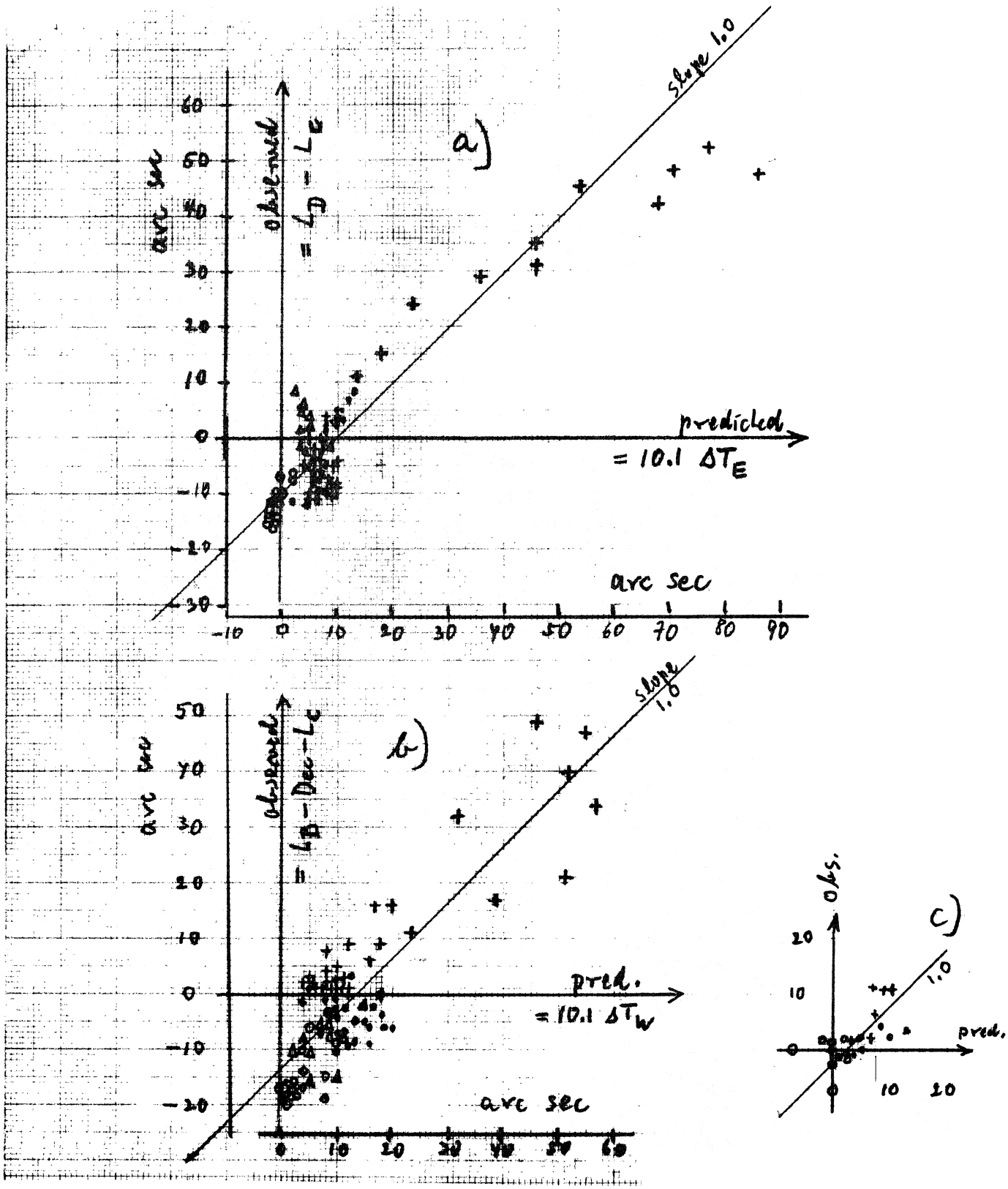

Fig. 6. Internal bending of yoke arms. Same symbols as in Fig. 5.
a) East arm, b) West arm, Nov. 10-14; c) Three maintenance days, East.

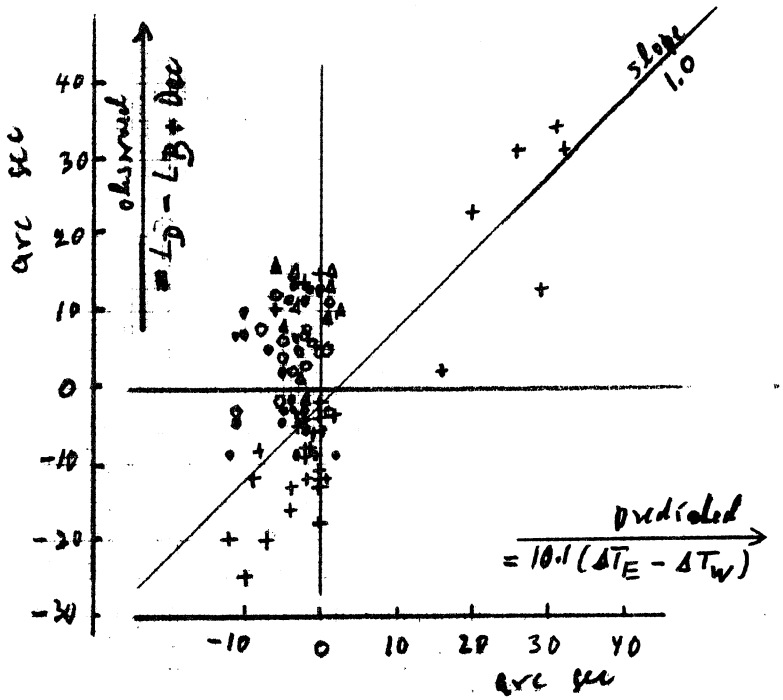

Fig. 7. Difference of yoke arm bendings, East - West.
Same symbols as in Fig. 5. Nov. 10-14.

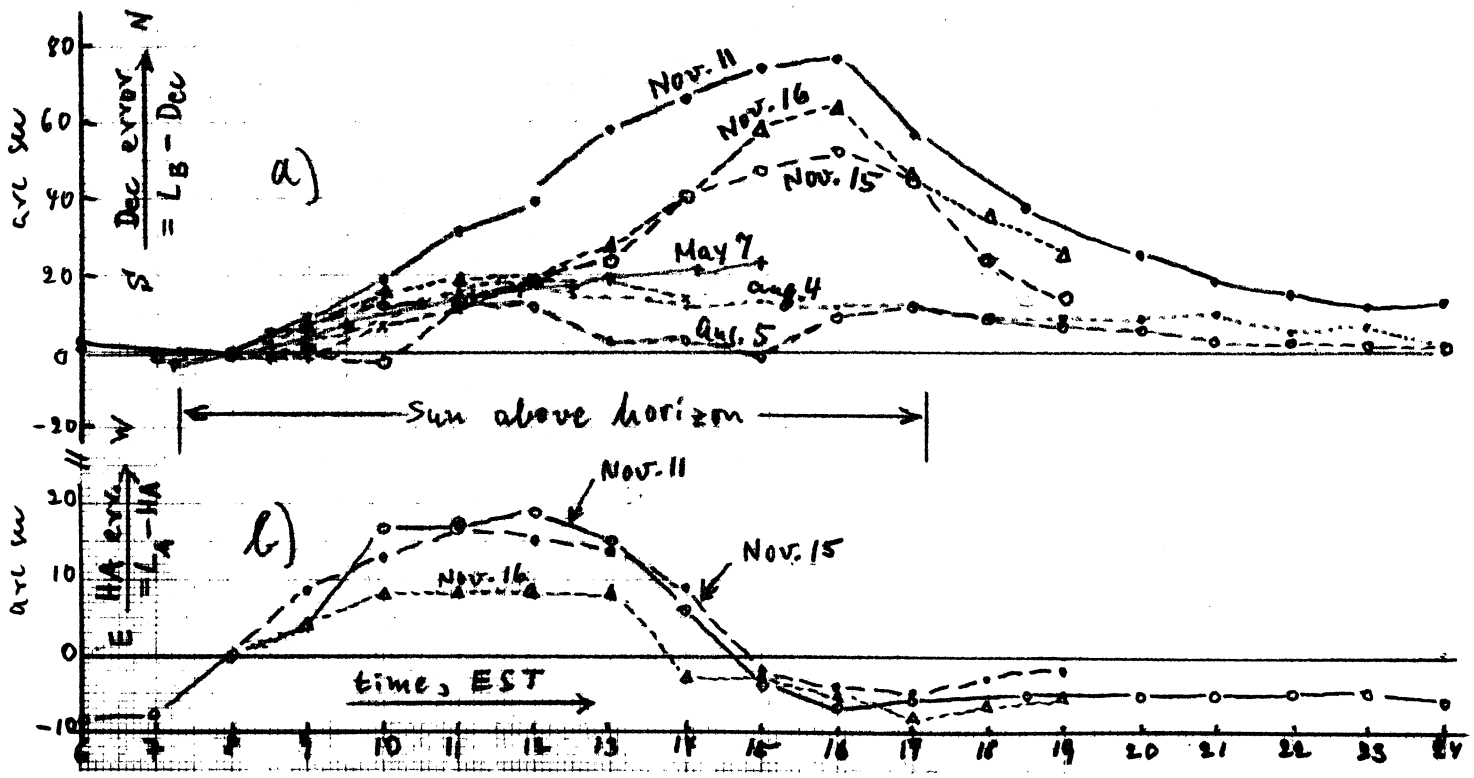

Fig. 8. Observed pointing errors, between center of declination axis (levels A, B) and console read-outs (Dec, HA). a) Declination; b) Hour angle.

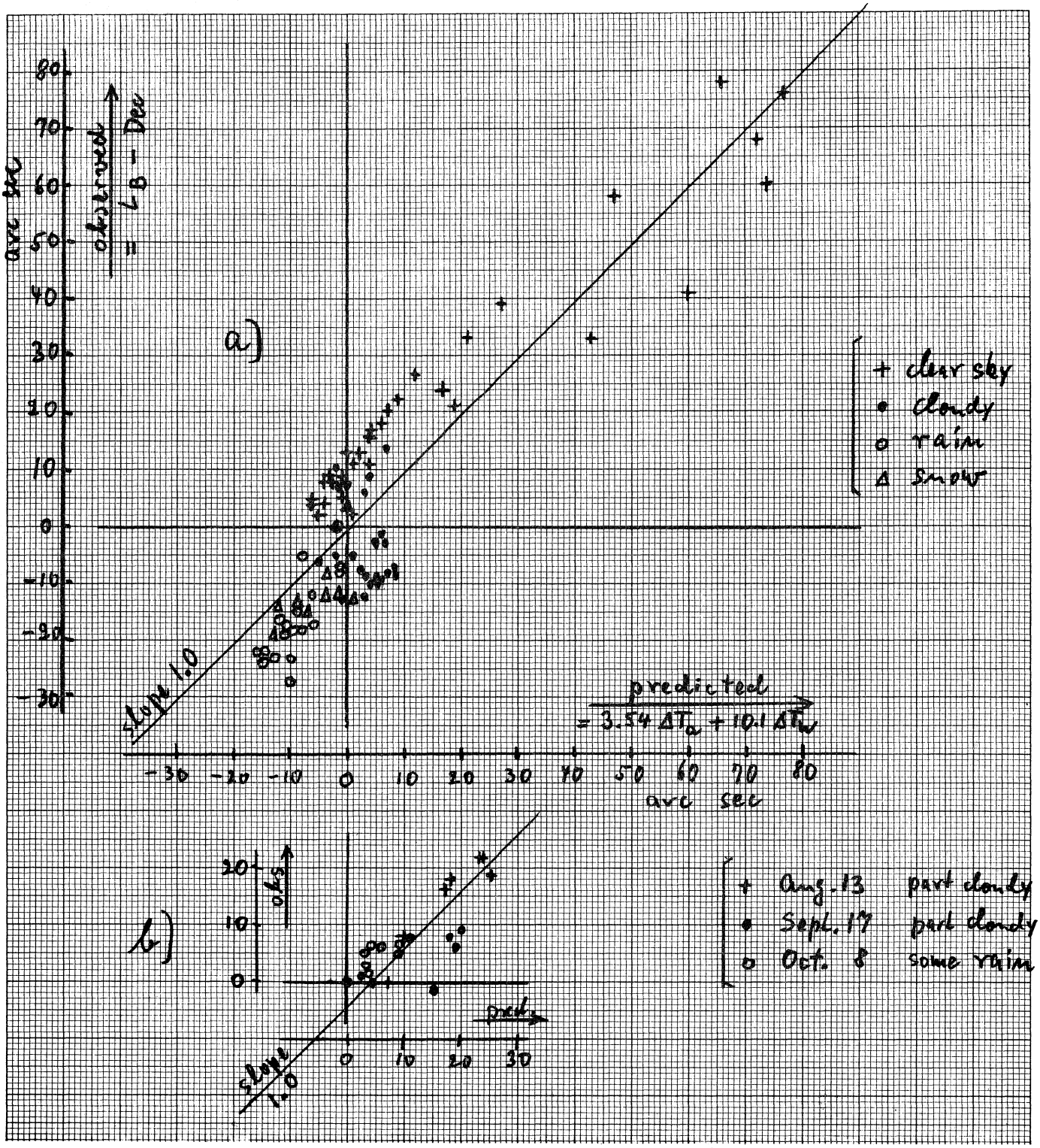

Fig. 9. Declination error, observed versus predicted.

a) Nov. 10-14; b) Three maintenance days.

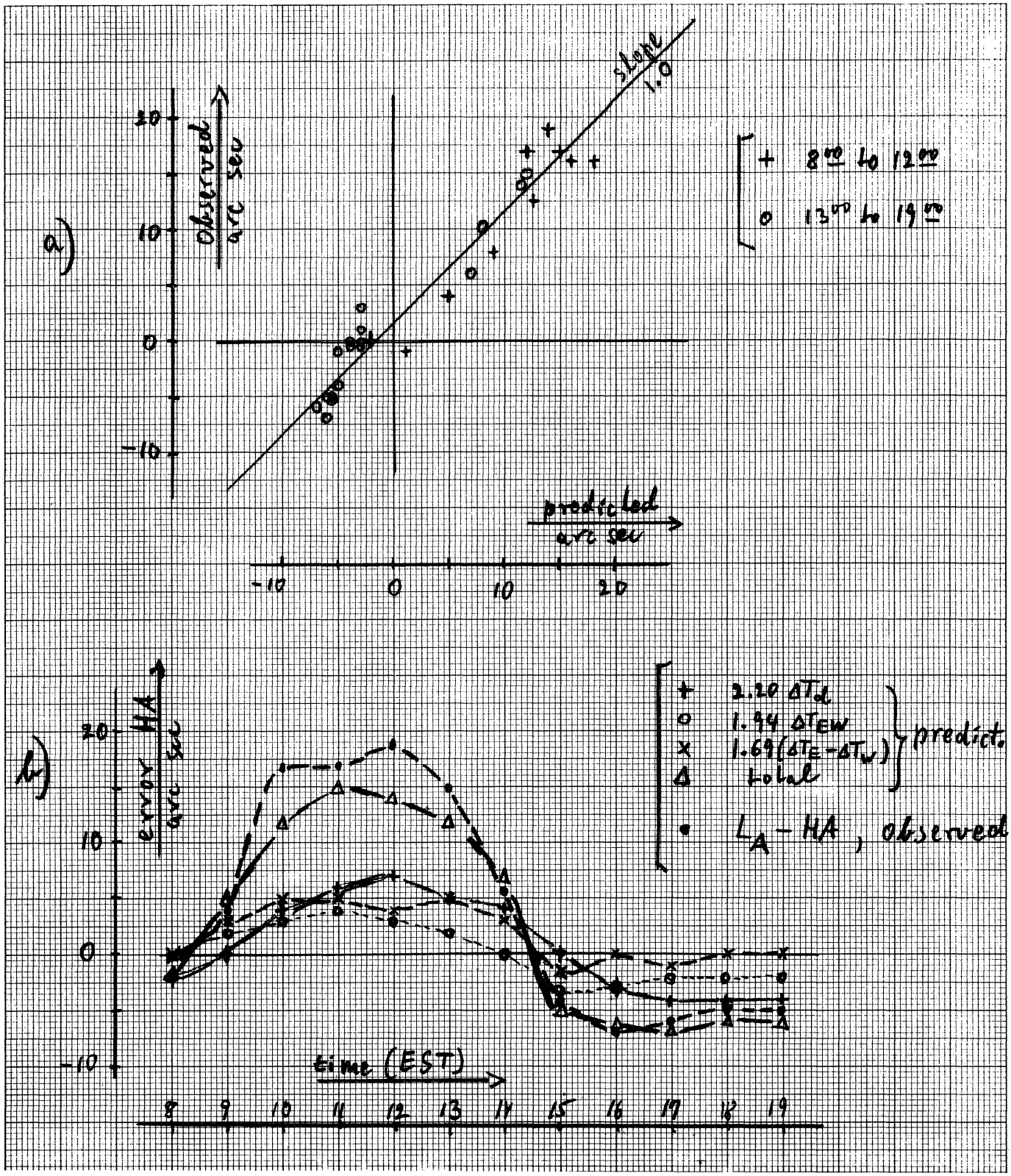

Fig. 10. Hour angle error.

a) Observed versus predicted, Nov. 11 and 19.

b) As function of time, three single contributions and total, Nov. 11.

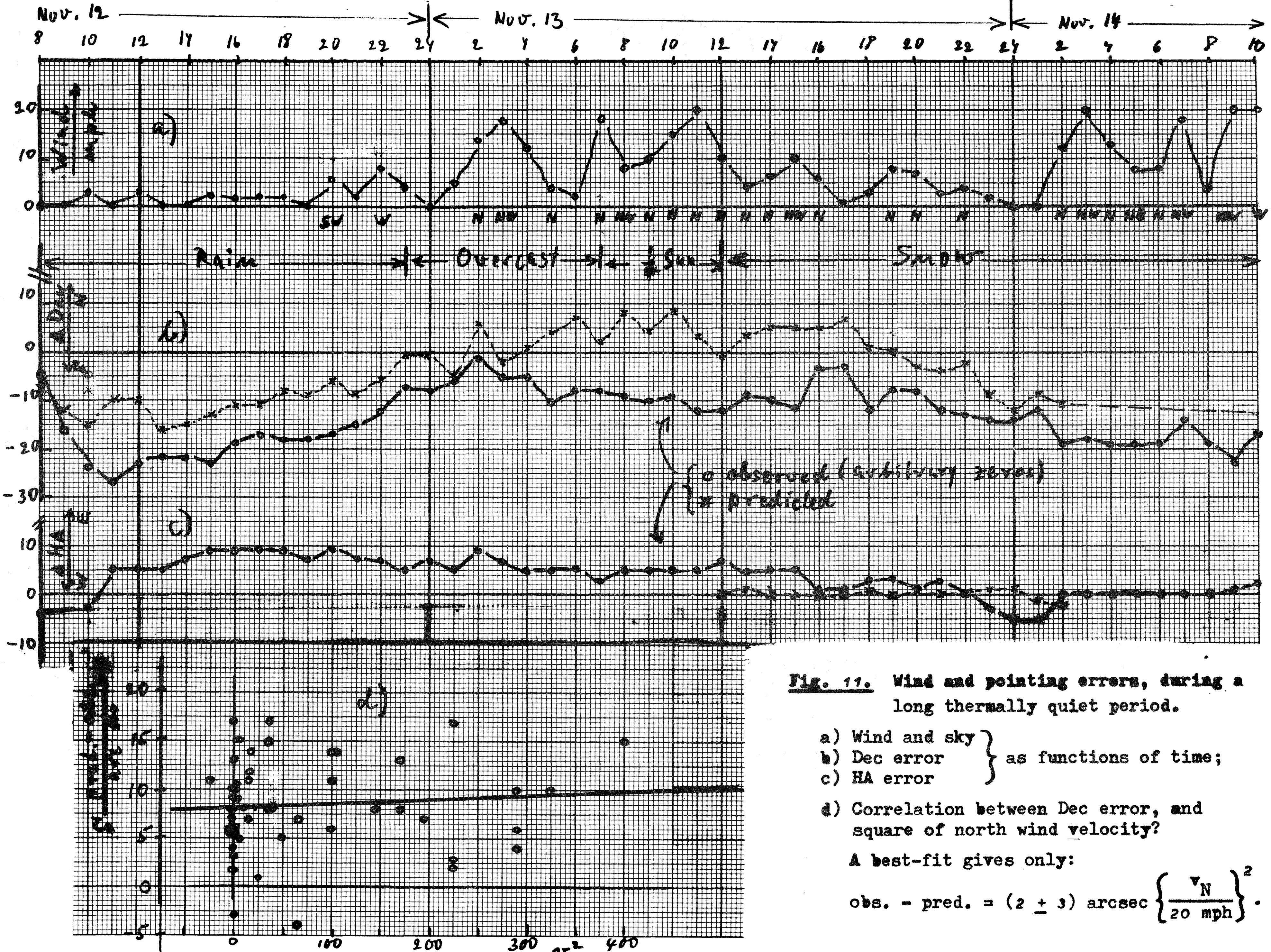

Fig. 11. **Wind and pointing errors, during a long thermally quiet period.**

a) Wind and sky
b) Dec error
c) HA error
} as functions of time;

d) Correlation between Dec error, and square of north wind velocity?

A best-fit gives only:

$$\text{obs.} - \text{pred.} = (2 \pm 3) \text{ arcsec} \left\{ \frac{v_N}{20 \text{ mph}} \right\}^2 .$$

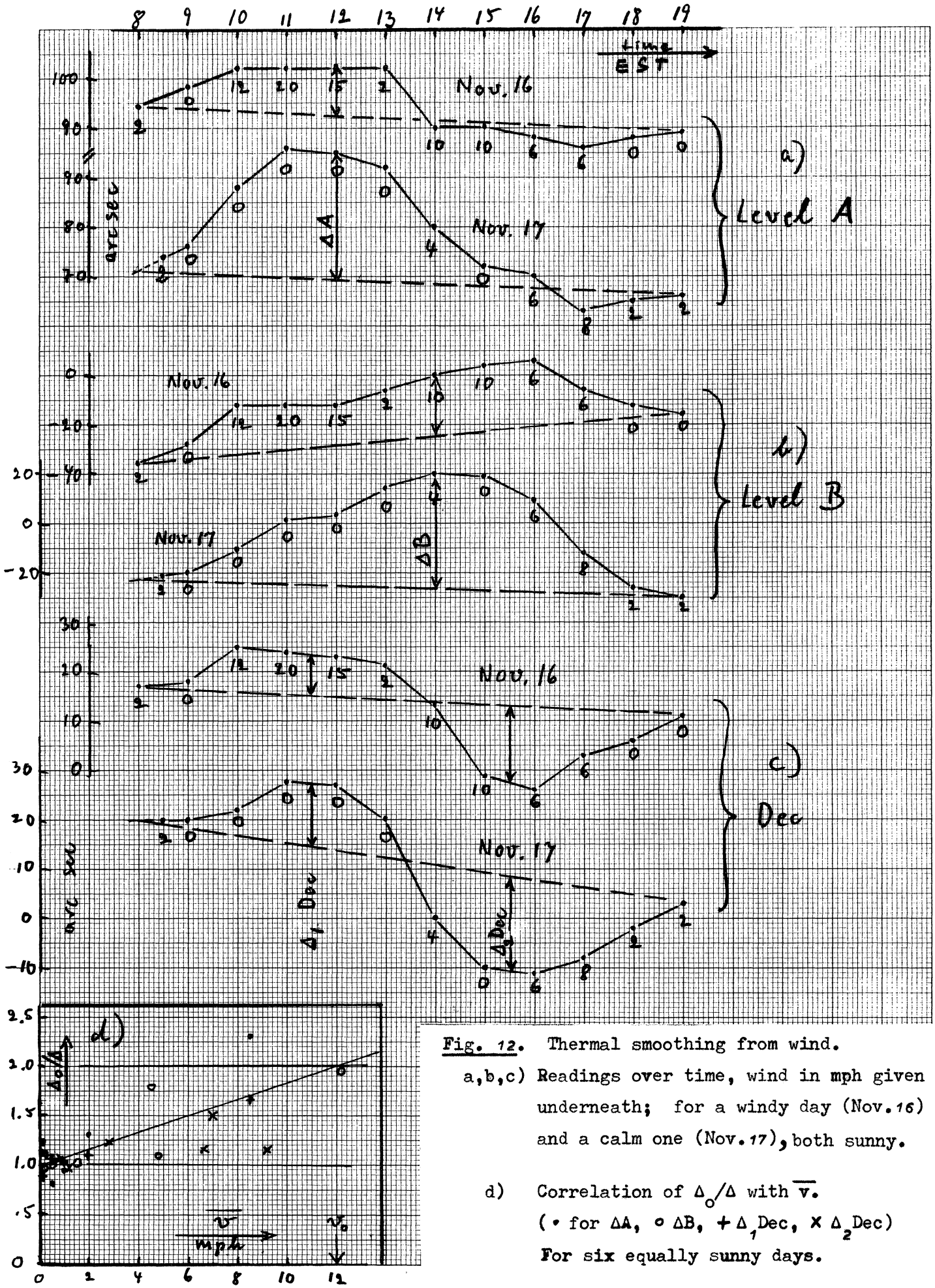

Fig. 12. Thermal smoothing from wind.

a,b,c) Readings over time, wind in mph given underneath; for a windy day (Nov. 16) and a calm one (Nov. 17), both sunny.

d) Correlation of Δ_o/Δ with $\bar{v}$.
(• for ΔA, ○ ΔB, + Δ_1Dec, × Δ_2Dec)
For six equally sunny days.